Asian Journal of Nanoscience and Materials 3 (2020) 226-237

Asian Journal of Nanoscience and Materials

Journal homepage: www.ajnanomat.com

Original Research Article

Strontium doped nanohydroxy apatite/reduced graphene oxide nanohybrid is speed up osteogenic differentiation of human mesenchymal stem cells

Shabnam Abedin Dargoush[a], Shadie Hatamie[b,*], Shiva Irani[a], Masoud Soliemani[d], Hana Hanaee-Ahvaz[c,*], Alireza Naderi Sohi[c]

[a] *Department of Biology, Science and Research Branch, Islamic Azad University, Tehran, Iran*

[b] *College of Medicine, National Taiwan University, 10048, Taipei, Taiwan*

[c] *Stem Cell Technology Research Center, Tehran, Iran*

[d] *Department of Hematology, Faculty of Medical Sciences, Tarbiat Modares University, Tehran, Iran*

ARTICLE INFORMATION

Received: 12 November 2019
Received in revised: 6 March 2020
Accepted: 15 March 2020
Available online: 17 May 2020

DOI: 10.26655/AJNANOMAT.2020.3.6

KEYWORDS

Reduced graphene oxide
Hydroxyapatite
Strontium
Adipose-derived mesenchymal stem cells
Osteogenic differentiation

ABSTRACT

Graphene based nanocomposites have been used to improve the osteogenic differentiation of stem cells. In this research study, the reduced graphene oxide (rGO) sheets were used as the base material while decorated with strontium doped hydroxyapatite (rGO/HAP/Sr). X-ray differentiation (XRD) analysis and transmission electron microscopy (TEM) were employed to evaluate the size and morphology of the HAP/Sr decorated rGO. Fourier transform infrared (FT-IR) was used to analyze the nanocomposites'functional groups. Raman spectroscopy was used to investigate the possible disorders in rGO/HAP/Sr structure and the number of layers. Ion-coupled plasma optical emission spectroscopy (ICP-OES) was used for evaluating the atomic concentrations of the elements (Ca and Sr) in nanocomposites. Likewise, zeta potential of the nanocomposite was determined to be -18.9 mV. To evaluate the cytotoxicity of the nanocomposites, MTT assay was performed. The osteo-inductive potential of the synthesized rGO/HAP/Sr nanocomposites was investigated using the adipose-derived mesenchymal stem cells (ADCs). Osteogenic differentiation was confirmed by measuring the calcium content. The results revealed that the nanocomposites concentrations induce calcium deposition by cells, indicating that the bone differentiation was done successfully. Lastly, it can be concluded that, this nanocomposite, alone, can be used for bone differentiation induction without using any chemical inducers.

Corresponding authors, email: hatamie@ntu.edu.tw & Hanaee@strc.ac.ir (Sh. Hatamie and H. Hanaee-Ahvaz).
Tel.: 00886966230784.

Graphical Abstract

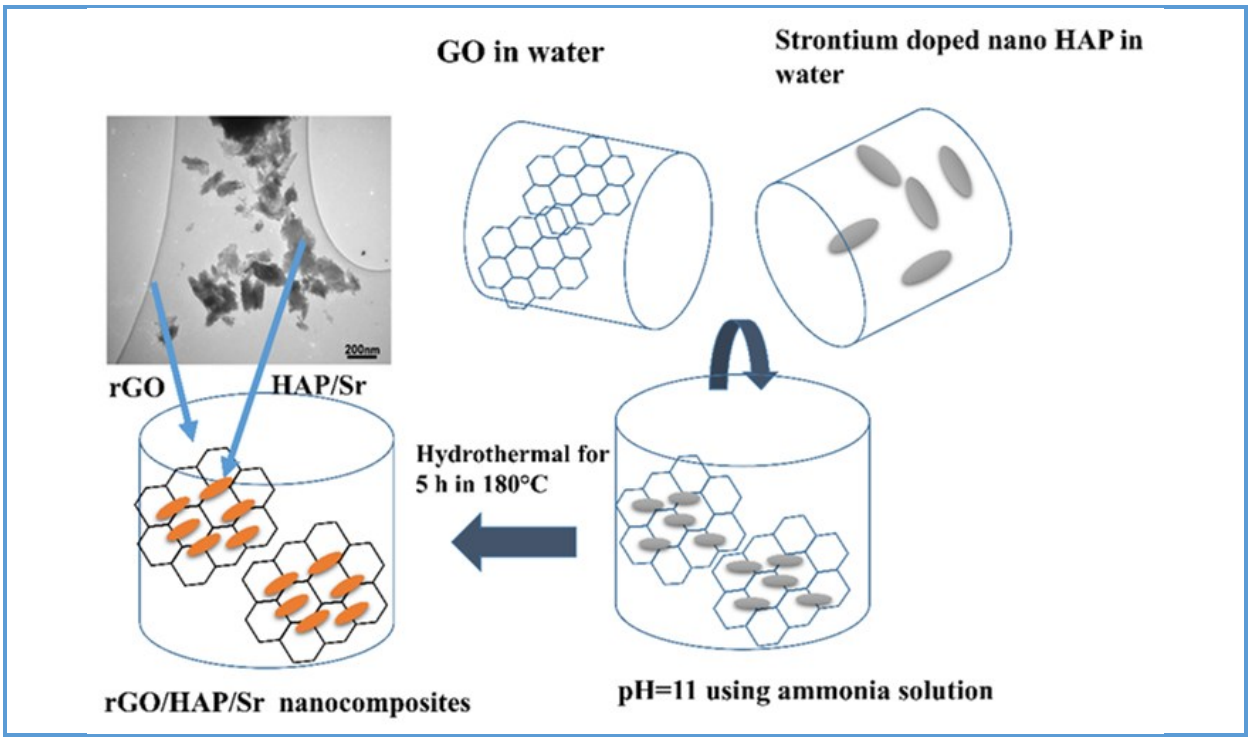

Introduction

Bone as a dynamic organ is responsible for repairing disrupted and old tissue. Furthermore, bone is an important supporting tissue of the body. It also protects the vital organs and the calcium and phosphate stores [1]. Tissue engineering has been created to combine the engineering with biological properties to create effective alternatives for diseased tissues. This is a promising for new clinical programs in the future [2]. Three main components in tissue engineering are scaffolds, stem cells, and growth factors. Scaffolds seeded by stem cells are designed to support the cell growth to construct a new tissue by the help of growth factors. Using nanotechnology techniques, structures could be built up as the same size as their natural form. Nanoparticles (NPs) are designed to modify scaffolds to reach better properties such as osteoinduction, ostecoduction and osteointegration properties [2, 3]. Different applications could be attributed to NPs in bone tissue engineering for gene and drug delivery to form the biomimetic scaffolds. Hydroxyapatite (HAP), calcium defective HAP (CDHAP) and tricalcium phosphate are known as bioceramic NPs that are biocompatible and have been used in biomedical uses [2, 4].

Hydroxyapatite ($Ca_{10}(Po_4)_6(OH)_2$ is one of the inorganic components of bone which because of its great bioactivity, biocompatibility and closeness to the natural bone, can support the bone regeneration and be utilized as a part of biomedical applications like, coating for fixation and filling material for bone imperfections [5–9]. In addition, HAP and B-tricalsium phosphate (B-TCP) are used widely as bone substituent due to their biocompatibility and osteoductivity [10]. One of the characteristic of the HAP which made it to be used as a scaffold in bone grafts is its very low absorption rate and its trabecular structure

that may help to introduce blood cells and bone cells for quicken bone deposition [11]. It was reported that, synthetic hydroxyapatite makes a problem in implants due to its low fracture toughness. Therefore, to improve its mechanical properties, hydroxyapatite has been doped with metal such as magnesium, zinc, strontium and manganese [12, 13].

Strontium (Sr) is one of the mineral elements of the bone, especially in the sections of the elevated metabolic turnover [14, 15]. Sr is aggregated in bone tissue and so it can be used as a marker for bone seeking because of its similarity to calcium [15–17]. The substitution of Sr in HAP makes its chemical structure more closely to the natural bone and enhances its biological, mechanical and antibacterial properties [17]. For instance, this substitution positively affects bone regeneration enhancement, bone resorption reduction [9] and potential in the treatment of osteoporosis. On the other hand, a study shows that adding strontium can reduces the risk of non-vertebral fractures in postmenopausal women with osteoporosis [18].

Graphene is one of the active carbon allotropes, where each carbon atom in the 2D crystal is bonded to the three other adjacent carbon atoms forming a hexagonal aromatic structure [7]. Graphene-based composites as a bioactive scaffold could enhance the differentiation of various stem cells towards specific families [26].

Incorporation of reduced graphene oxide (rGO) sheets with HAP could increase osteo differentiation of mesenchymal stem cells (MSCs) without preventing their proliferation [19]. These ontogenesis promotions are examined by early stage marker of osteo differentiation such as alkalin phosphatase activity and calcium mineralization as late stage marker. Moreover, rGO/HAP grafts were used in full-thickness calvarial defects in order to enhance new bone regeneration without any inflammatory responses [20, 21]. So, it is suggested that rGO/HAP have ability to promote osteogenesis and in conclude could accelerate bone regeneration. The aim of this study was to synthesize novel nanocomposites which represent or might boost up the osteoinductive capacity of rGO, Sr and HAP which compensate the negative characteristics (such as low mechanical characteristics for Hap). The rGO/HAP/Sr nanocomposites were synthesized using hydrothermal method and characterized using XRD, TEM, Raman spectroscopy and FTIR methods. The nanocomposites biocompatibility and potential in osteogenic differentiation of ADCs were investigated.

Experimental

Materials and method

Graphite powder (mesh≤200 μm), potassium permanganate (KMnO4), sulfuric acid (H_2SO_4), sodium nitrate ($NaNO_3$), hydrogen peroxide (H_2O_2), calcium nitrate ($Ca(NO_3)_2$), strontium nitrate ($Sr(NO_3)_2$), di-ammonium hydrogen phosphate $NaH_2(PO_4)_2$, of Merck were used in the chemical fabrication process, without further purification. DMEM, FBS, Dexamethasone, β-glycerol phosphate, ascorbic acid bisphosphate of Sigma as well as Abdominal adipose tissue were used in cellular part.

Preparation of rGO

Graphene oxide (GO) was prepared using the graphite powder as a source, through modified Hummers' method [30]. In this method, 0.5 g of graphite powder and 0.5 g of sodium nitrate (NaNO3) were dissolved in 23 mL of sulfuric acid at 0 °C. Then, 3 g of $KMnO_4$ was gradually added to the mixture, followed by heating up to

35 °C. The temperature was kept constant and the mixture was stirred for 4 h. After the reaction was completed, 40 mL of water was added drop-wise to the solution. Then, 100 mL of water and 3 mL H_2O_2 were added to the solution to complete the process. The color of the mixture turns into bright yellow, as GO is formed. The suspension was filtered and washed with HCl and deionized water twice, followed by washing by deionized water once more to tune the pH to 5. Finally, the aqueous solution of graphite oxide was ultra-sonicated several times to exfoliate to form GO. GO is most commonly reduced by chemical methods using reducing agents such as hydrazine, and thermal treatments in order to remove the oxygen-containing functional groups.

Construction of Sr doped HAP

0.7 g of $NaH_2(PO_4)_2$, 1.18 g of $Ca(NO_3)$ and 0.5 g $Sr(NO_3)$ were dissolved in 10 mL, 5 mL and 5 mL of distilled water, respectively. The Sr solution was added drop-wise to calcium nitrate solution to adjust the PH to 11. Then, the $NaH_2(PO_4)_2$ was added to the mixture and the reaction was completed by stirring the solution for 5 h at room temperature. The synthesized material centrifuged at 3000 rpm for 10 min. Then the precipitate was dried in oven and collected.

Preparation of rGO sheets decorated by HAP/Sr

0.1 g of HAP/Sr and GO were dissolved in 40 mL of DI water in different flasks. Then, the HAP/Sr solution was gently poured to aqueous GO solution and the resulting mixture was stirred for 15 min. The PH of the mixture was adjusted to 11 using the ammonia solution. Finally, the solution was transferred in Teflon line stainless steel autoclave and placed in oven for 5 h. Then the sample was centrifuged and washed with DI water. In each washing step, the supernatant was discarded till PH was tuned to 7. The resultant was dried in oven in 50 °C for 24 h.

Nanocomposites characterization technique

Fourier transform infrared (FT-IR) spectra were obtained using the Bruker spectrometer. The samples were prepared by grinding dried powder of rGO/HAP/Sr with KBr. The grinded material was then compressed into thin pellets. This test was performed using Almega Thermo Nicolet Dispersive Raman spectrometer, with excitation laser wavelength of 532 nm. TEM images were acquired using a transmission electron microscopy (JEOL JEM-2010) at 200 kV. The specimens for TEM were prepared by placing the aqueous suspension of rGO/HAP/Sr on carbon-coated copper grids. XRD patterns were recorded using the AXS Bruker diffractometer, with the CuKα radiation of wavelength of 0.154 nm. The ICP-OES was used to find the percentage of the HAP/Sr loading in the nanocomposites, using Spectro Arcos instrument. The rGO/HAP/Sr are dispersed in sodium phosphate buffer (PBS) at pH~7 and zeta potential was measured by a Malvern Instrument Ltd-UK. Dispersions were determined by the electrophoresis with Zetasizer 3000 by Malvern.

Cell isolation

Abdominal adipose tissue was obtained from the patients after obtaining the patient's written consent according to the ethics of Tehran University of Medical Sciences. Cell isolation was carried out according to [22]. Briefly, the tissue was washed with PBS containing Penicillin/Streptomycin, and then digested with 150 µg/mL collagenase type I (Sigma) for 40 min (5% CO_2 at 37 °C). After neutralization and treatment with RBC lysis buffer, cells were centrifuged and incubated at 37 °C, 5% CO_2.

Culture medium contained 10% FBS, Penicillin (100 U/mL)/Streptomycin (100 µg/mL). In all experiments cells were used at 3-7 passages.

Cell viability test using MTT assay

Cytotoxicity assay of rGO/HAP/Sr nanocomposites (NCs) was studied using MTT assay. Mesenchymal stem cells (MSCs, 3×10^3 cells/cm^2) were seeded in each of 96-well plates and then cultured in 200 µL of DMEM supplemented with 10% FBS and 1% penicillin. Moreover, different concentrations NCs (1 µg/mL, 3 µg/mL, 5 µg/mL, 7 µg/mL, 10 µg/mL) were added to each well to evaluate cytotoxicity in 3 time points of day 1, day 3, day 7. After 3 h of incubation in MTT solution, dimethyl sulfoxide was added into each of the wells and optical density was read at 570 nm (BioTek instruments, USA).

Osteogenic differentiation

For osteogenic differentiation, cells at passages 3-9 at density of 5000 cells/cm^2 were seeded on TCPS plate. At 80% of confluence, cells received osteogenic medium (OM group, DMEM, 10% FBS, 10^{-7} M Dexamethasone, 10 mM b-glycerol phosphate, 50 µg/mL ascorbic acid bisphosphate). Other test group received nanocomposites at determined concentration (1-10 µg/mL) for 14 days. Cells which received no osteogenic treatments served as control group.

Calcium deposition measurements

For calcium content measurement for each treatment, calcium deposition test was performed. Cells were homogenized in 0.6 N HCL (Merck) and centrifuged with 1200 rpm for 5 min. The released calcium was determined using calcium assay kit (Pars Azmoon). The optical density was read at 570 nm (BioTek instruments, USA). Finally, the data was normalized against total protein for all groups. Total protein measurements were carried out using BCA kit (Life Technologies) according to manufacturer instruction.

Statistical analysis

Statistical analyses were carried out using SPSS software and one-way analysis of variance (ANOVA) to compare the results. Gene expression data were analyzed by REST 2009 software. A P value of<0.05 was considered to be statistically significant. All test was done in duplicate.

Results and Discussion

TEM images

TEM images of nanohybride are shown in Figure 1**a**, **b** , the rGO sheets have approximately 2-3 µm sizes and the HAP/Sr composites are decorated the rGO surfaces. As seen in Figure 1, the HAP/Sr nanocomposites have rod shapes with the internal diameter of 100 nm with the length of approximate 200 nm. The rGO sheets are mostly seems to be mono layer.

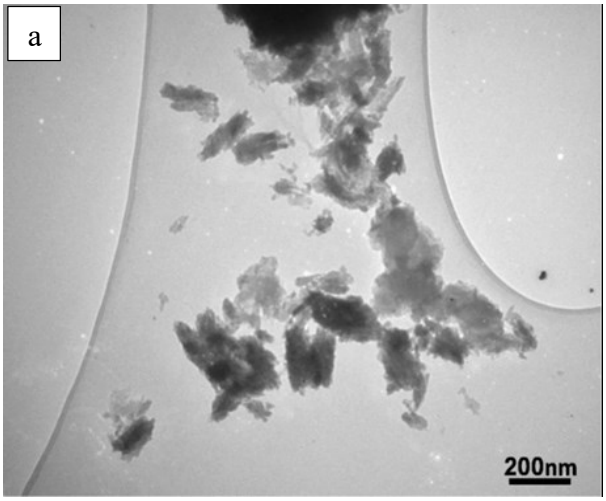

rGO/HAP/Sr structure study

The Figure 2a, presents the XRD patterns for rGO/ HAP/Sr nanocomposite. The Figure

2a, presents the XRD patterns for rGO/HAP/Sr nanocomposite.

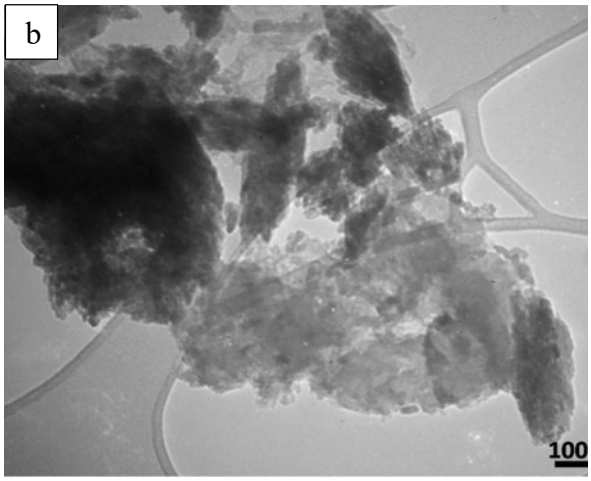

Figure 1. TEM images of the rGO/HAP/Sr nanocomposites

As seen in Figure 2**a**, the XRD characteristic peaks are corresponding to that of calcium HAP (JCPDS no.09-0432) and strontium hydroxyapatite (JCPDS no. 33-1348). It is proved that the effect of the incorporation Sr^{2+} in HAP are shifted the XRD peaks to the lower 2θ, and increase in peak intensities., which is regarding to the expansion of HAP crystal lattice, and more effect X-ray scattering of strontium compared to the calcium respectively. Furthermore, the characteristic peak of rGO should place at 25 degrees are diminished, which can be regarding to the amorphous nature of the graphene and the incorporation of the HAP/Sr on the graphene sheets are weakened the graphene sheets diffraction pattern. Another reason could also be small amount of the rGO sheets and decrease on the peak intensity compart to the nearest peak of HAP/Sr [45].

The FT-IR spectra of the as synthesized rGO/HAP/Sr nanocomposites is shown in Figure 2**b**. The bands which are placed at 1022.3, 1223.03, 1449.92, 589.407, 553.438 cm^{-1} are attributed to the PO_4^{3-} of HAP [25]. The bonds at 3448.63 and 1568.39 cm^{-1} are corresponding to strongly adsorbed of H_2O [26]. Typical hydroxyl bands appears at 3448.63 cm^{-1} which is characteristic for apatite containing higher concentration of CO_3^{2-} per unit cell [27].

Raman spectroscopy was used to investigate the possible dis-orders in graphene structure , to find the number of its layer [28, 29], and to determine the attachments of the HAP/Sr on the rGO sheet surfaces. Figure 2c, shows Raman spectra of the rGO/HAP/Sr monohybrids. The double band positions corresponding to the G and D bonds of graphitic structures are observed in the Raman spectrum. The typical G peak position for single layer carbon materials are reported to be at 1580 cm^{-1} for single layer graphene sheets, but here it is slightly shifted to 1585 cm^{-1}, which means of more layer of graphene than one. The I_D/I_G ratio of graphene sheets could be stand for sp^2 domain size in graphitic fabrication which comprises of sp^2 and sp^3 bonds. In this study, the nanocomposite I_D/I_G is estimated to be 0.84 cm^{-1} in the wavelength of 532 nm, which is decreased compare to the GO, which shows the reduction of GO to rGO form. The I_{2D}/I_G ratio are shows the number of the reduced graphene oxide sheets. For the rGO/HAP/Sr sample this ratio is calculated to be ~ 0.11 cm^{-1}, which is shown the multi-layer structure (approximate 4 layers) of rGO.

Ion-coupled plasma optical emission spectroscopy (ICP-OES) was used to find the atomic concentrations of elements (Ca and Sr) in the rGO/HAP/Sr nanocomposites. The amount of the Sr and Ca are reported to be 7 and 10 weight percent (wt%) respectively in the nanocomposites which means the maximum amount is for the reduced graphene oxide. Then this results show that the graphene materials occupied approximate 80 wt% of the nanocomposites.

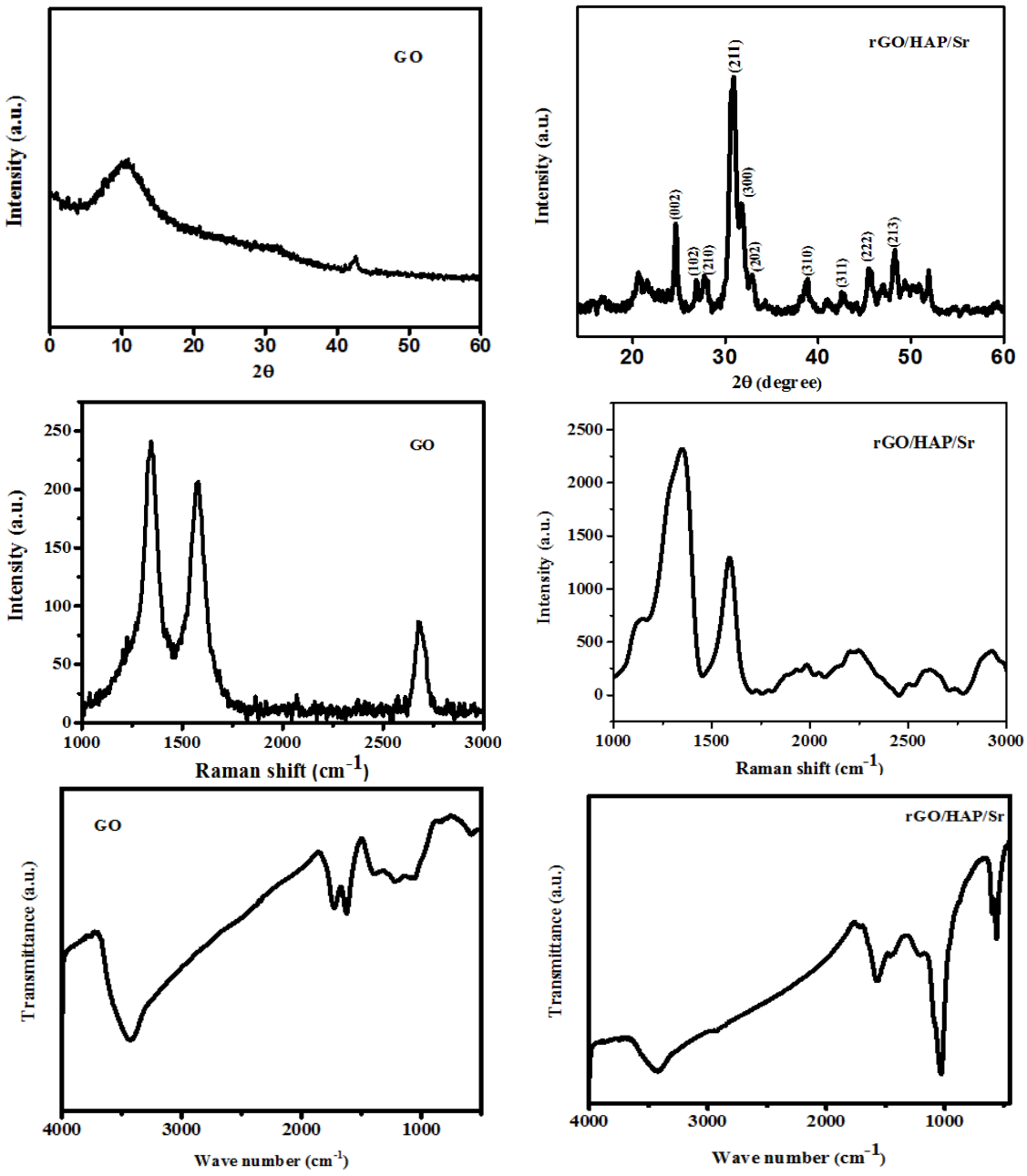

Figure 2. XRD and FT-IR and Raman spectroscopy of GO, and rGO/HAP/Sr nanocomposites

The Zeta potential of nanocomposites was obtained to be -18.9 mV which is increased compared to the GO zeta potential which is -40 mV. It could be corresponding to the removing of oxygen functional groups on the GO sheet surfaces and the attached of the positive HAP/Sr in the rGO surfaces.

Cytotoxicity measurements

To obtain the optimum concentration of NCs for osteogenesis induction, the cytotoxicity of NCs was studied at different concentrations through 7 days using MTT assay. Figure 3, represents the various biological responses of the cells to different dosage of NCs. Overall it

can be seen that there is no toxicity of nanocomposites in cells in all studied concentrations of NCs in days 1 and 3, but at longer time points (day 7) slight cytotoxicity was observed for concentration 3 µg/mL onwards. Accordingly, for prolonged treatment of cells with this NCs, concentration lower than 5 µg/mL is recommended. However, the decrease in cell proliferation which observed for higher NCs concentrations might be due to ultimate osteogenic differentiation of the cells that occurred in shorter time range.

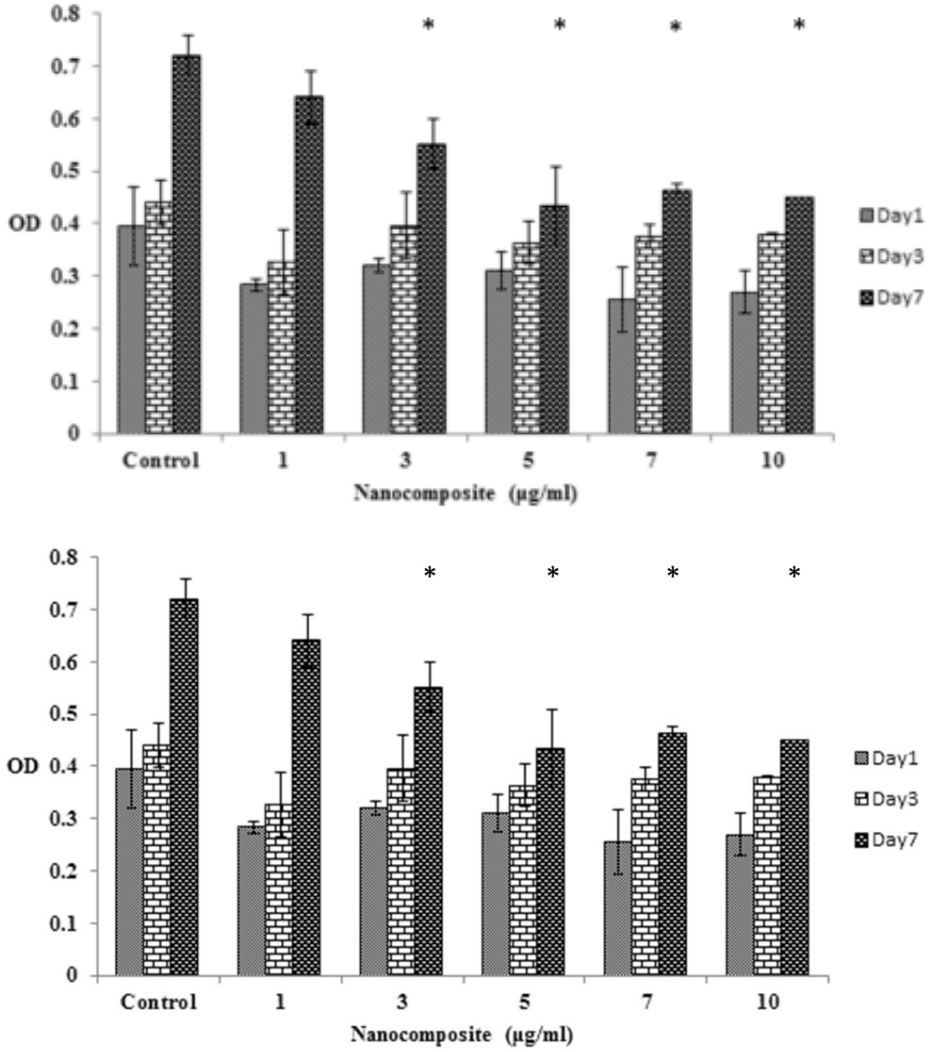

Figure 3. MTT assay. Cell viability in control (no treatment) vs different concentrations of nanocomposites. "* $p<0.05$" indicate significant differences between each concentration in comparison with its own control

Calcium deposition

Calcium content as marker of osteo-induction capability of each treatment was measured. As presented in Figure 4., in comparison to control and OM group, NCs in all concentration, led to calcium deposition and osteogenic differentiation. Additionally, more calcium deposition was observed when cells have been treated with higher NCs

concentration. Induction of differentiation with osteogenic medium led the highest calcium deposition. Furthermore, based on our results, NCs treatment is solely enough to induce osteogenic differentiation in cells. In addition, in range of 5 to 10 µg/mL of NCs, no significant difference was observed in amount of deposited calcium. The effect of HAP in nanocomposites for calcium content measurement was subtracted.

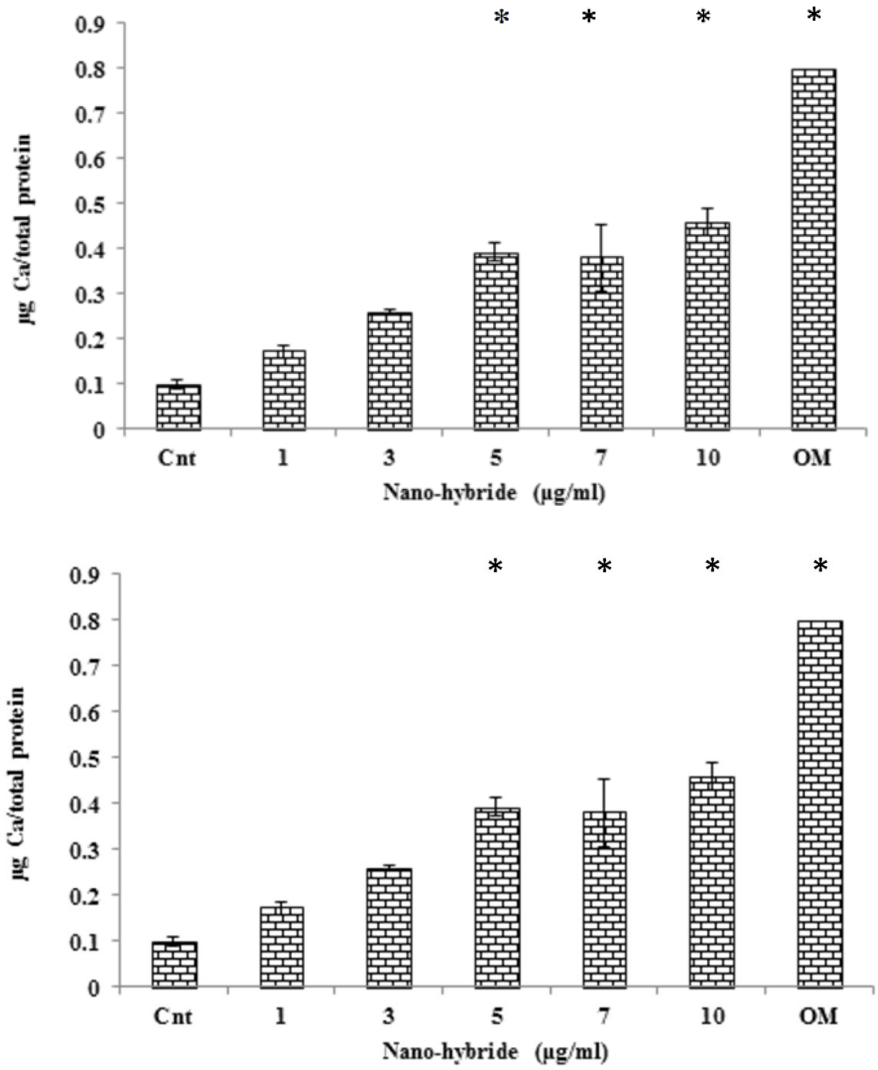

Figure 4. Calcium deposition. In comparison to control (CNT) and OM (Osetogenic Medium) group, nanocomposites (NCs) in all concentration, led to calcium deposition and osteogenic differentiation. ''* $p<0.05$'' indicate significant differences

Bone is a dynamic organ which can replace the old or disintegrated tissue through a remodeling process. This process is essential for bones to match the mechanical changes of the skeleton under different environmental conditions [1]. Bone remodeling is the balance of activity between two different groups of cells, osteoclasts and osteoblasts, which are involved in bone resorption and deposition, respectively [30]. Tissue engineering and regenerative

medicine are the new research fields that evaluate how organs and tissues are regenerated through natural signaling pathways and components of the organism, such as stem cells and growth factors [30-32]. Bone tissue renovation is one of the main challenges in the field of tissue engineering and regenerative medicine. Anatomical complications of bone, with high mechanical stress it is exposed, made it a unique texture that is almost impossible to replicate [2].

In recent years, the use of nanoparticles in the field of tissue engineering, biotechnology, and biomedicine has increased substantially. One of the main reasons is that the nanoparticles, as compared to traditional medicine have the potential to create new technology applications [33]. Different nanoparticles current used on bone tissue engineering research are consist of organic (Lyposomes, polymeric NPs, Dendrimers) and inorganic (Silica NPs, Gold NPs, Magnetic NPs, Ceramic NPs, Carbon nanotubes, Quantum Dots) [2]. In this study, the reduced graphene oxide (rGO) sheets were used as the base material while decorated with strontium doped hydroxyapatite (rGO/HAP/Sr) and osteo-inductive potential of the synthesized rGO/HAP/Sr nanocomposites was investigated using adipose-derived mesenchymal stem cells (ADCs).

The electron confinement in the graphene orbitals is localized to neighboring carbon atoms to create the covalent σ-bonds. The σ-bonds (C-C bonds) are responsible for the perfectly planar nature of graphene, determining its strong mechanical properties. The unique electrical, mechanical and physical properties of the graphene such as its higher hardness than the diamond, thermal conductivity near thirteen times higher than copper, elastic modulus as high as 1 Tpa, and good optical transparency of around 97.7% transmittance cause to be blended with other polymers and materials to reinforce their characteristics [7]. In addition, overlapping other orbital electrons and π-planar densities on both sides of the graphene sheets high surfaces are created π- bond between each pair of adjacent carbon atoms [34]. Graphene can also be easily combined with the bioactive compounds such as proteins, enzymes, drugs, growth factors, and DNA *via* physical interaction [7, 35, 36]. Strontium containing biomaterials are being increasingly developed for orthopedic applications. The release of strontium from the biomaterial surface in the physiological environment is believed to promote cell proliferation, differentiation and enhance the metabolic activity of osteoblasts [24].

Previous studies have shown that low doses of strontium increase bone mineralization and high doses have a negative effect [39, 40]. The molecular mechanism is not well understood, although various *in vitro* studies have illustrated that Sr-doping in HAP causes osteoblasts' differentiation as well as proliferation by activating calcium sensing receptor, which leads to both osteogenesis and angiogenesis stimulation [41]. studies have also reported that strontium ions can stimulate osteoblasts [43, 44] and down-regulate the osteoclast activity. According to previous studies, the use of reduced graphene oxide (rGO) sheets with HAP has been shown to increase osteodifferentiation of Mesenchymal stem cells (MSCs) without preventing their proliferation [19]. Therefore, as strontium has a significant contribution to bone mineralization, we have combined these materials and monitored effects of constructed nanocomposites on cells osteogenic differentiation.

In our study, it can be seen that there is no toxicity of nanocomposites in cells in all the

studied concentration of NCs after 3 days; however, at longer time, points slight time dependent cytotoxicity was observed for concentration higher than 5 μg/mL. Accordingly, for prolonged treatment of cells with this NCs, concentration lower than 5 μg/mL is recommended. The toxicity of the graphene depends on the concentration, particle size, functionalization, and exposure time [37]. Many of studies have suggested that a high concentration (100) of graphene induces toxicity [24, 38]. Calcium deposition, as the last stage of differentiation, can be a marker for bone differentiation [2].

Conclusions

This work illustrated the osteogenesis of adipose-derived mesenchymal stem cells that was stimulated spontaneously by rGO/HAP/Sr NCs without using any osteoinductive agents. The deposition of calcium phosphate in the extracellular matrix is suggestive of osteogenesis and is taken as a marker for bone regeneration. It was observed that NCs treatment was individually enough to induce osteogenic differentiation in cells, furthermore, an increase in the NCs concentration led to elevating the calcium deposition in cells. Besides, there was no significant difference in the amount of deposited calcium when NCs in the range of 5 to 10 μg/mL were used. Moreover, various characterization techniques were applied to examine the properties of the synthesized nanocomposites. Biocompatibility of the nanocomposites was approved by the cytotoxicity assay. Also, no cytotoxicity was observed by the nanocomposites at any concentrations in day 1 and 3, although in longer periods (day 7) minor toxicity was detected for concentrations 3 μg/mL onwards.

Disclosure Statement

No potential conflict of interest was reported by the authors.

References

[1]. Valenti M., Dalle Carbonare L., Mottes M. *International Journal of Molecular Sciences*, 2016, **18**:41
[2]. Vieira S., Vial S., Reis R.L., Oliveira J.M. *Biotechnology Progress*, 2017, **33**:590
[3]. Roohani-Esfahani S.I., Nouri-Khorasani S., Lu Z.F., Appleyard R.C., Zreiqat H. *Acta Biomaterialia*, 2011, **7**:1307
[4]. Gaharwar A.K., Dammu S.A., Canter A.M., Wu C.J., Schmidt G. *Biomacromolecules*, 2011, **12**:1641
[5]. Boanini E., Gazzano M., Bigi A., *Acta Biomaterialia*, 2010, **6**:1882
[6]. Cox S.C., Jamshidi P., Grover L.M., Mallick K.K. *Materials Science and Engineering: C*, 2014, **35**:106
[7]. Shin S.R., Li Y.C., Jang H.L., Khoshakhlagh P., Akbari M., Nasajpour A., Shrike Zhang Y., Tamayol A., Khademhosseini A. A*dvanced Drug Delivery Reviews*, 2016, **105**:255
[8]. Landi E., Celotti G., Logroscino G., Tampieria A. *Journal of the European Ceramic Society*, 2003, **23**:2931
[9]. Devi Ravi N., Balu R., Sampath Kumar T.S. *Journal of the American Ceramic Society*, 2012, **95**:2700
[10]. Huang X., Zeng Z., Fan Z., Liu J., Zhang H. *Advanced Materials*, 2012, **24**:5979
[11]. Peón Avés E., Fuentes G. Delgado J., Morejon Alonso L., Almirall A., Carrodeguas R. *Latin American Applied Research*, 2004, **34**:225
[12]. Kim H.W., Koh Y.H., M., Kong Y.M., Kim H.E. *Journal of Materials Science: Materials in Medicine*, 2004, **15**:1129
[13]. Sopyan L., Mardziah C.M., Toibah A.R., Singh R. *Advanced Materials Research*, 2008, **47-50**:928
[14]. Tredwin C.J., Young A.M., Abou Neel E.A., Georgiou G., Knowles J.C. *Journal of Materials Science: Materials in Medicine*, 2013, **25**:47
[15]. Özbek Y.Y., Baştan F.E., Üstel F. *Journal of Thermal Analysis and Calorimetry*, 2016, **125**:745

[16]. Tredwin C.J., Young A.M., Abou Neel E.A., Georgiou G., Knowles J.C. *Biomaterials*, 2005, **26**:4073
[17]. Capuccini C., Torricelli P., Boanini E., Gazzano M., Giardino R., Bigi A. *Journal of Biomedical Materials Research Part A*, 2009, **89A**:594
[18]. Reginster J.Y., Seeman E., De Vernejoul M.C., Adami S., Compston J., Phenekos C., Devogelaer J.P., Diaz Curiel M., Sawicki A., Goemaere S., Sorensen O.H., Felsenberg D., Meunier P.J. *The Journal of Clinical Endocrinology & Metabolism*, 2005, **90**:2816
[19]. Holt B.D., Wright Z.M., Arnold A.M., Sydlik S.A. *Interdisciplinary Reviews: Nanomedicine and Nanobiotechnology*, 2017, **9**:e1437
[20]. Lee J.H., Shin Y.C., Jin O.S., Kang S.H., Hwang Y.S., Park J.C., Hong S.W., Han D.W. *Nanoscale*, 2015, **7**:11642
[21]. Li J.L., Tang B., Yuan B., Sun L., Wang X.G. *A Biomaterials*, 2013, **34**:9519
[22]. Pakfar A., Irani S., Hanaee-Ahvaz H. *Tissue and Cell*, 2017, **49**:122
[23]. Xu C., Wang X., Zhu J., Yang X., Lu L. *Journal of Materials Chemistry*, 2008, **18**:5625
[24]. Kumar S., Chatterjee K., *Nanoscale*, 2015, **7**:2023
[25]. Ning Z., Chang Z., Li W., Sun C., Zhang J., Liu Y. *Chinese Journal of Chemical Engineering*, 2012, **20**:89
[26]. Suganthi R.V., Elayaraja K., Joshy M.I.A., Chandra V.S., Girija E.K., Kalkura S.N. *Materials Science and Engineering*: C, 2011, **31**:593
[27]. Prekajski M., Mirković M., Todorović B., Matković A., Marinović-Cincović M., Luković J., Matović B. *Journal of the European Ceramic Society*, 2016, **36**:1293
[28]. Dresselhaus M.S., Jorio A., Hofmann M., Dresselhaus G., Saito R. *Nano Letters*, 2010, **10**:751
[29]. Tuinstra F., Koenig J.L. *The Journal of Chemical Physics*, 1970, **53**:1126
[30]. Cancedda R., Dozin B., Giannoni P., Quarto R. *Matrix Biology*, 2003, **22**:81
[31]. Kashef-Saberi M.S., Hayati Roodbari N., Parivar K., Vakilian S., Hanaee-Ahvaz H. *ASAIO Journal*, 2018, **64**:e115
[32]. Kazem-Arki M., Kabiri M., Rad I., Roodbari N.H., Hosseinpoor H., Mirzaei S., Parivar K., Hanaee-Ahvaz H. *Cytotechnology*, 2018.
[33]. Tautzenberger, A., Kovtun, and Ignatius, Nanoparticles and their potential for application in bone. *International Journal of Nanomedicine*, 2012: p. 4545.
[34]. Liu L., Zhang J., Zhao J., Liu F. *Nanoscale*, 2012, **4**:5910
[35]. Weaver C.L., Cui X.T. *Advanced Healthcare Materials*, 2015, **4**:1408
[36]. Liu Z., Liu B., Ding J., Liu J. *Analytical and Bioanalytical Chemistry*, 2014, **406**:6885
[37]. Akhavan O., Ghaderi E., Akhavan A., *Biomaterials*, 2012, **33**:8017
[38]. Chang Y., Yang S.T., Liu J.H., Dong E., Wang Y., Cao A., Liu Y., Wang H. *Toxicology Letters*, 2011, **200**:201
[39]. Egles C., Ehret C., Aid-Launais R., Sagardoy T., Siadous R., Bareille R., Rey S., Pechev S., Etienne L., Kalisky J., de Mones E., Letourneur D., Amedee Vilamitjana J. *Plos One*, 2017, **12**:e0184663
[40]. Frasnelli M., Cristofaro F., Sglavo V.M., Dirè S., Callone E., Ceccato R., Bruni G., Cornaglia A.I., Visai L. *Materials Science and Engineering: C*, 2017, **71**:653
[41]. Chattopadhyay N., Quinn S.J., Kifor O., Ye C., Brown E.M. *Biochemical Pharmacology*, 2007, **74**:438
[42]. Xue W., Moore J.L., Hosick H.L., Bose S., Bandyopadhyay A., Lu W.W., Cheung K.M.C., Luk K.D.K. *Journal of Biomedical Materials Research Part A*, 2006, **79A**:804
[43]. Sharma L., Kapoor D., Issa S. *Current Opinion in Rheumatology*, 2006, **18**:147
[44]. Qiu K., Zhao X.J., Wan C.X., Zhao C.S., Chen Y.W. *Biomaterials*, 2006, **27**:1277
[45]. Edwin N., Saranya S., Wilson P. *Ceramics International*, 2019, **45**:5475

How to cite this manuscript: Shabnam Abedin Dargoush, Shadie Hatamie*, Shiva Irani, Masoud Soliemani, Hana Hanaee-Ahvaz*, Alireza Naderi Sohi. Strontium doped nanohydroxy apatite/reduced graphene oxide nanohybrid is speed up osteogenic differentiation of human mesenchymal stem cells. *Asian Journal of Nanoscience and Materials*, 3(3) 2020, 226-237. DOI: 10.26655/AJNANOMAT.2020.3.6